



A Deformable Template Model, with Special Reference to Elliptical Templates

ASGER HOBOLTH, JAN PEDERSEN AND EVA B. VEDEL JENSEN

Department of Mathematical Sciences, University of Aarhus, Ny Munkegade, DK-8000 Aarhus C, Denmark

Abstract. This paper suggests a high-level continuous image model for planar star-shaped objects. Under this model, a planar object is a stochastic deformation of a star-shaped template. The residual process, describing the difference between the radius-vector function of the template and the object, is allowed to be non-stationary. Stationarity is obtained by a time change. A parametric model for the residual process is suggested and straightforward parameter estimation techniques are developed. The deformable template model makes it possible to detect pathologies as demonstrated by an analysis of a data set of cell nuclei from a benign and a malignant tumour, using stochastic deformations of ellipses.

Keywords: deformable template model, ellipse, Fourier analysis, non-Gaussian errors, non-stationarity, shape, time change

1. Introduction

In high-level image modelling, the objects of an image are modelled directly. A very useful class of models is the deformable template models suggested by Ulf Grenander and the group around him, cf. e.g. [2–4]. The basic idea is to model the observed object as a stochastic deformation of a template. The challenging task is to describe the deformation mechanism.

Deformable template models for featureless planar objects have attracted a lot of attention in the statistical literature recently, cf. e.g. [3, 4, 6, 7, 10, 13, 14]. The focus has mainly been on circular templates. In the present paper we suggest a deformable template model for a random star-shaped planar object K which is useful in the case of non-circular templates. The radius-vector function $R = \{R(t)\}_{t \in [0,1]}$ of K is modelled as $R(t) = r(t) + X(t)$ where $r(t)$ is the deterministic radius-vector function of the template and $X(t)$ is a random residual process. For non-circular templates it is not natural to assume that $X(t)$ is stationary. We therefore introduce a time change $\gamma(t)$ such that $X_0(t) = X(\gamma^{-1}(t))$ is stationary. This is a generalization of the approach described in [15], p. 90.

Modelling of $X_0(t)$ is based on a Fourier expansion. For elliptical templates it is assumed that the Fourier coefficients of $X_0(t)$ at the phases $s = 0, 1, 2$ are small. The remaining Fourier coefficients are modelled as normal random variables with mean zero and variance λ_s at phase s given by the regression equation

$$\lambda_s^{-1} = \alpha + \beta(s^{2p} - 3^{2p}), \quad s \geq 3,$$

where α, β, p are unknown parameters. We discuss how the parameters influence the random geometry of the object and consider various choices of time changes.

In [5] elliptical templates were also studied, but the approach deviates significantly from ours as will be discussed in Sections 3 and 4. The papers [6, 7, 10, 16] are based on Fourier expansions of either the tangent-angle function or the radius-vector function. The statistical models proposed in these papers describe a circular rather than an elliptical shape.

In Section 2 we define the general model. Various distributional results will be provided when X_0 is Gaussian and extensions to the non-Gaussian case will be discussed. In Section 3 we specialize to elliptical

templates. The suggested model is used in the analysis of a data set concerning cancer diagnostics in Section 4.

2. A Deformable Template Model

Let a random planar object K be star-shaped relative to $z \in K$ such that K is determined by the radius-vector function $R = \{R(t)\}_{t \in [0,1]}$ with respect to z , where

$$R(t) = \max\{u : z + u(\cos 2\pi t, \sin 2\pi t) \in K\}, \quad t \in [0, 1].$$

Note that $R(t)$ is the distance from z to the boundary of K in the direction $2\pi t$. For a detailed description of the radius-vector function, see [7] and references therein.

We suppose that the radius-vector function of K is on the form

$$R(t) = r(t) + X(t), \quad t \in [0, 1], \quad (2.1)$$

where $r = \{r(t)\}_{t \in [0,1]}$ is the radius-vector function of the template and $X = \{X(t)\}_{t \in [0,1]}$ is a residual process which is periodic and has mean zero. For a circular template with z at the centre of the circle, $r(t)$ is constant and equal to the radius of the circle.

We assume that there exists an increasing transformation γ of $[0, 1]$ onto $[0, 1]$ such that $\{X(\gamma^{-1}(t))\}_{t \in [0,1]}$ is stationary. In particular, the correlation between $X(\gamma^{-1}(t_1))$ and $X(\gamma^{-1}(t_2))$ depends on $t_2 - t_1$ only. We say that X is γ -stationary. In the stochastic process literature γ is referred to as a time change, cf. e.g. [12], and we will use the same terminology.

The choice of γ is important. When the template is a circle, then the only reasonable choice of γ is the identity, $\gamma(t) = t$, in which case the correlation between $X(t_1)$ and $X(t_2)$ depends only on $t_2 - t_1$. However, for a non-circular template the identity may be a poor choice. For instance, for an elliptical template, the distance between two boundary points at angles $2\pi t_1$ and $2\pi t_2$, respectively, will for fixed $t_2 - t_1 = \Delta$ be smaller near the minor axis than near the major axis, cf. Fig. 1(a). Therefore, it is not natural in this case to assume that the correlation between $X(t_1)$ and $X(t_2)$ depends on $t_2 - t_1$ only. An obvious choice of $\gamma(t)$ for a general template is the distance travelled on the boundary of the template between the points with index 0 and t , $t \in [0, 1]$. With this choice of γ , the correlation between $X(t_1)$ and $X(t_2)$ only depends on the distance along the tem-

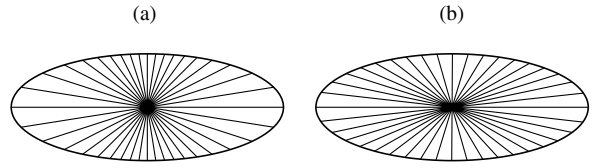


Figure 1. In (a), points on the boundary of an ellipse with constant angle $2\pi\Delta$ between neighbour points are plotted while in (b) the distance along the boundary between neighbour points is constant.

plate boundary between the points indexed by t_1 and t_2 , cf. Fig. 1(b).

We can rewrite (2.1) as

$$R_0(t) = r_0(t) + X_0(t), \quad t \in [0, 1],$$

where $R_0(t) = R(\gamma^{-1}(t))$ and similarly for the other quantities. Note that $X_0 = \{X_0(t)\}_{t \in [0,1]}$ is stationary in the ordinary sense.

We suppose that the residual process is Gaussian. Let

$$r_0(t) = a_0 + \sqrt{2} \sum_{s=1}^{\infty} a_s \cos(2\pi st) + \sqrt{2} \sum_{s=1}^{\infty} b_s \sin(2\pi st)$$

and

$$X_0(t) = A_0 + \sqrt{2} \sum_{s=1}^{\infty} A_s \cos(2\pi st) + \sqrt{2} \sum_{s=1}^{\infty} B_s \sin(2\pi st) \quad (2.2)$$

be the Fourier expansions of r_0 and X_0 . Under the Gaussian assumption for X_0 , A_0 and $A_s, B_s, s \geq 1$, are all mutually independent, $A_0 \sim N(0, \lambda_0)$ and $A_s \sim B_s \sim N(0, \lambda_s), s \geq 1$. It follows that the Fourier expansion of R_0 has the same distributional properties as those of X_0 , except that zero mean-values are substituted by the relevant Fourier coefficients from the template.

To summarize, in order to specify the model we have to decide on (i) the template, determined by its radius-vector function r , (ii) the time change γ and (iii) a model for the variances λ_s . Once we have decided on (i)–(iii), the process X_0 determines the deviation of the object from the template. At small frequencies s the Fourier coefficients A_s and B_s determine the ‘global’

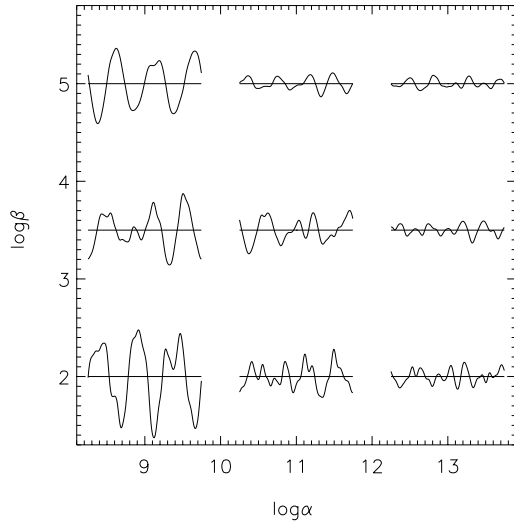


Figure 2. Simulations of the residual process X_0 , obtained when the variances are of the form $\lambda_s^{-1} = \alpha + \beta(s^{2p} - 3^{2p})$, $s \geq 3$. The values of the parameters α and β are as indicated and $p = 2.5$. A high global fluctuation in X_0 is seen when α is small (corresponding to large λ_s for small s). The local fluctuation in X_0 is high when β is small (corresponding to large λ_s for large s). The parametric model for the $\lambda_{s,s}$ is discussed in detail in Section 3.

behaviour of X_0 , cf. Fig. 2. That is, if the variances λ_s for small s are high, then there will typically be a high fluctuation in X_0 , meaning that K deviates from the template in ‘global’ shape. Conversely, if λ_s is small when s is small then the shape of K resembles the shape of the template. Similarly, at high frequencies, A_s and B_s control the ‘local’ behaviour of X_0 . High variances λ_s give an object with an ‘irregular’ boundary, and small variances a more ‘smooth’ boundary.

Whether λ_s is large or small, must be judged relative to the so-called phase amplitudes c_s of the template. To see this, let us consider a polar Fourier expansion of R_0 . Letting

$$\begin{aligned} a_0 + A_0 &= \sqrt{C_0} \\ a_s + A_s &= \sqrt{2C_s} \cos(2\pi s D_s), \\ b_s + B_s &= \sqrt{2C_s} \sin(2\pi s D_s), \quad s \geq 1, \end{aligned}$$

we get

$$\begin{aligned} R_0(t) &= a_0 + A_0 + \sqrt{2} \sum_{s=1}^{\infty} (a_s + A_s) \cos(2\pi s t) \\ &\quad + \sqrt{2} \sum_{s=1}^{\infty} (b_s + B_s) \sin(2\pi s t) \end{aligned}$$

$$\begin{aligned} &= \sqrt{C_0} + 2 \sum_{s=1}^{\infty} \sqrt{C_s} \cos(2\pi s(t - D_s)), \\ &\quad t \in [0, 1], \end{aligned}$$

with phase amplitude $C_s \geq 0$ and phase angle $D_s \in [0, 1/s)$. Under the Gaussian assumption, we have that C_0 and (C_s, D_s) , $s \geq 1$, are all independent and the observed phase amplitudes

$$C_s = \begin{cases} (a_0 + A_0)^2 & s = 0 \\ ((a_s + A_s)^2 + (b_s + B_s)^2)/2 & s \geq 1, \end{cases}$$

follow non-central χ^2 -distributions with expectations given by

$$\begin{aligned} EC_0 &= E(a_0 + A_0)^2 = a^2 + \lambda_0 = c_0 + \lambda_0 \\ EC_s &= E((a_s + A_s)^2 + (b_s + B_s)^2)/2 \\ &= (a_s^2 + b_s^2)/2 + \lambda_s = c_s + \lambda_s, \quad s \geq 1, \end{aligned}$$

respectively, where c_s is the s th phase amplitude of the template. Thus, if $c_s \gg \lambda_s$ the observed phase amplitude C_s is mainly determined by the template and if $c_s \ll \lambda_s$ mainly by the residual process. In fact, the distribution of C_s can for $s \geq 1$ be approximated by a $(c_s + \lambda_s)\chi^2(f_s)/f_s$ -distribution where

$$f_s = 2 \left(1 + \frac{c_s^2}{\lambda_s^2 + 2c_s\lambda_s} \right),$$

cf. e.g. [8]. Note that for a circular template, we have $c_s = 0$, $f_s = 2$ and the result is exact. If $c_s \gg \lambda_s$, then f_s will be large and the distribution of C_s is concentrated around c_s .

The conditional distribution of D_s given C_s is, cf. the Appendix,

$$2\pi s D_s | C_s = c \sim vM \left(2\pi s d_s, 2 \frac{\sqrt{cc_s}}{\lambda_s} \right), \quad s \geq 1, \quad (2.3)$$

where $d_s \in [0, 1/s)$ is the s th phase angle of the template. Here, $vM(\mu, \kappa)$ is the notation used for the von Mises distribution with mean direction $\mu \in [0, 2\pi)$ and concentration parameter $\kappa \geq 0$. For $\kappa = 0$ we get the uniform distribution on $[0, 2\pi)$ while for $\kappa > 0$ large the distribution is concentrated around the mean direction. Other properties of this distribution are described in [11], p. 36. From (2.3) it is seen that if $c_s \gg \lambda_s$ then D_s is concentrated around the template phase angle d_s .

while if $c_s \ll \lambda_s$ then D_s can be regarded as uniformly distributed on $[0, 1/s)$ which is the distribution of the phase angle from the residual process.

If the template is a circle, then $a_s = b_s = 0 = c_s, s \geq 1$. Using that A_0 and $A_s, B_s, s \geq 1$, are all independent normally distributed as indicated above, C_s and D_s are independent, C_s follows an exponential distribution with mean λ_s and D_s is uniformly distributed on $[0, 1/s), s \geq 1$.

The distributional results obtained above for (C_s, D_s) in the Gaussian case motivate extensions of our model to the non-Gaussian case. Instead of the $(c_s + \lambda_s)\chi^2(f_s)/f_s$ -distribution one might use a generalized gamma distribution as a model for C_s , cf. [9], Section 8.4. Under a Gaussian assumption the phase angles are von Mises distributed as indicated in (2.3). An extension is here to consider a von Mises distribution of the type $vM(2\pi s d_s, \kappa_s \sqrt{c})$ where the parameter $\kappa_s > 0$ is arbitrary, allowing for larger and smaller variation than in the Gaussian case. However, we shall not pursue this possibility further in the present paper.

3. Elliptical Templates

From now on we consider the special case where the template is an ellipse.

Let us start by introducing some notation for an ellipse. Assume the centre z is located at the origin, let the lengths of the axes be denoted by $a \geq b$ and the eccentricity by $\epsilon = (1 - b^2/a^2)^{1/2}$. If the major axis of the ellipse has an angle of $2\pi\theta$ relatively to the first axis, $\theta \in [0, 1/2)$, then the boundary of the ellipse is given by

$$(x(t), y(t)) = r(t)(\cos(2\pi t), \sin(2\pi t)), \quad t \in [0, 1],$$

where the radius-vector function is

$$r(t) = \frac{ab}{\sqrt{a^2 \sin^2(2\pi(t - \theta)) + b^2 \cos^2(2\pi(t - \theta))}}. \tag{3.1}$$

The boundary length between the points with indices 0 and t is

$$l(t) = \int_0^t \sqrt{(x'(u))^2 + (y'(u))^2} du \\ = 2\pi ab \int_{-\theta}^{t-\theta} \frac{(a^4 \sin^2(2\pi u) + b^4 \cos^2(2\pi u))^{1/2}}{(a^2 \sin^2(2\pi u) + b^2 \cos^2(2\pi u))^{3/2}} du. \tag{3.2}$$

The time change γ will be taken to be either the relative boundary length, $\gamma(t) = l(t)/l(1)$, or the identity, cf. Fig. 1. In both cases one easily shows that at odd phases the time changed radius-vector function $r_0(t) = r(\gamma^{-1}(t))$ has vanishing Fourier coefficients. In fact, if the eccentricity is not too large then the elliptical shape is mainly determined by the Fourier coefficients at the phases $s = 0$ and $s = 2$ for these two choices of time change.

Recall that the time changed radius-vector function R_0 of the random object K is $R_0(t) = r_0(t) + X_0(t)$. We want to specialize the general Gaussian model for X_0 such that K has a pronounced elliptical shape. As noted above this should be reflected in the Fourier coefficients at phases $s = 0$ and $s = 2$. We assume that X_0 has small Fourier coefficients when $s = 0$ and $s = 2$ such that at these phases R_0 is described almost entirely by the terms from the ellipse. Moreover, typically K will be rather symmetrical with respect to the centre z , and arguing as in Section 2 of [7] this implies that the Fourier coefficients of R_0 at phase $s = 1$ are small.

We hence consider the Gaussian model (2.2) with variances $\lambda_0, \lambda_1, \lambda_2$ small. The remaining variances are modelled by the simple regression model

$$\lambda_s^{-1} = \alpha + \beta(s^{2p} - 3^{2p}), \quad s \geq 3. \tag{3.3}$$

The parameter α determines the ‘global’ deviation from the template while β, p determine the ‘roughness’ of the boundary. The reason is that when $s \geq 3$ is small then λ_s is mainly determined by α . In particular, $\lambda_3 = \alpha^{-1}$. A small value of α gives a large value of λ_s which typically implies a high ‘global’ fluctuation in $X_0(t)$, cf. Section 2. Similarly when s is large λ_s is merely determined by β and p . Large values of these parameters yield small variances λ_s such that the boundary of K will be rather smooth, see Fig. 2. In [7] it is discussed how p relates to continuity and differentiability of the trajectories of X_0 , see in particular Section 3 of that paper. In particular, it is shown that if X_0 is Gaussian and the template boundary is arbitrary smooth, the radius-vector function of the random object K is $k - 1$ times continuously differentiable where k is the integer satisfying $p \in [k - 1/2, k + 1/2]$. The regression model is called a p -order model because it appears as the limit of discrete time p -order Markov models, cf. [7]. The limit is obtained by considering an appropriate p -order Markov model for n points on the object boundary and then let $n \rightarrow \infty$.

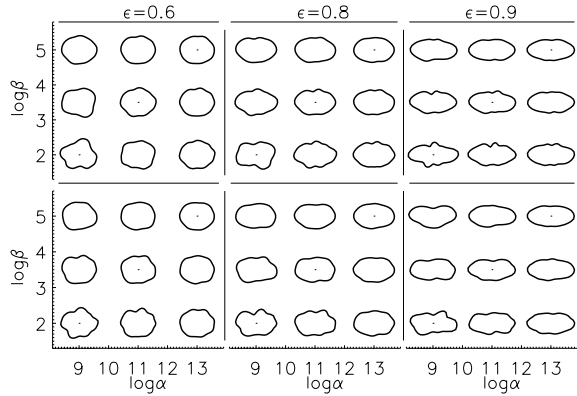


Figure 3. Simulations from the model (2.2) with $A_s = B_s = 0$, $s \leq 2$, λ_s given by (3.3) and an elliptical template with unit perimeter. In the first three rows the time change is $\gamma(t) = t$ while in the last three rows $\gamma(t) = l(t)$. The values of ϵ , α and β are as indicated and $p = 2.5$.

In the statistical shape literature a Gaussian model is commonly used, cf. e.g. [3–7, 10, 13–15]. The papers [6, 7, 10] considered Gaussian models with Fourier coefficients at phase $s = 0, 1$ close to zero. The additional constraint on $s = 2$ here is due to the choice of template. Compared to [6, 7, 10] we have also introduced the time change γ . In [5] a template ellipse was considered but the constraints on the Fourier coefficients were not incorporated.

An effective way of checking that a model has the right properties is to inspect random samples from the model. In Fig. 3 we show simulations using both $\gamma(t) = t$ and $\gamma(t) = l(t)/l(1)$. All templates were scaled such that the perimeter was $l(1) = 1$. For $\epsilon = 0$ the two time changes are identical and therefore yield the same model. However, at high eccentricities it is apparent that $\gamma(t) = t$ results in some undesirable small ‘blobs’ in K near the minor axis of the template ellipse. The small blobs are indeed expected because, if γ is the identity, then the correlation between points on the boundary of K is smaller at the minor axis than at the major axis, cf. also Fig. 1(a). In the following we will therefore mainly use $\gamma(t) = l(t)/l(1)$ as our time change.

4. Data Analysis

The data consists of 27 profiles of cell nuclei from a malignant tumour and 27 cell nuclei from a benign tumour of human skin, cf. Fig. 4 and ref. [5], where the data has previously been analysed. The cell nuclei

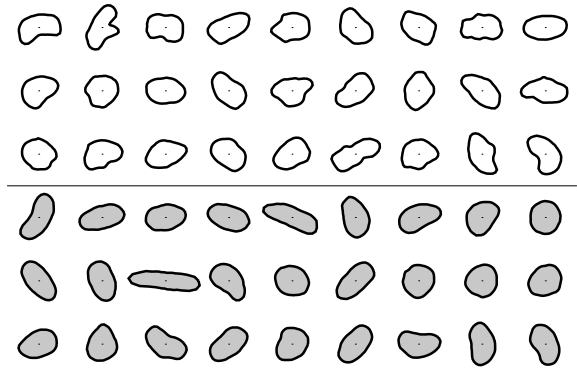


Figure 4. The upper panel is profiles of cell nuclei from a malignant tumour while the lower is from a benign tumour. The cell nuclei have been scaled so that they have approximately the same size.

from the benign tumour seem to be small deformations of ellipses with varying eccentricities while the nuclei from the malignant tumour are larger deformations of ellipses. The deformable elliptical model should be able to capture this difference.

For each profile we chose z as the centre of mass and calculated the radius-vector function R at the points $t = 0, 1/n, \dots, (n-1)/n$, where $n = 50$. We tried several different ways of fitting the ellipse. The elegant method described in [1] was implemented, the least squares method described in [5] was also used, but we ended up fitting the ellipse using the Fourier coefficients at the phases $s = 0, 2$ only. However, the three methods resulted in almost the same template ellipse.

Since we are only interested in the shape we scaled the resulting residual process $X(t) = R(t) - r(t)$ by the perimeter of the ellipse. Finally we calculated the Fourier coefficients of the normalized time changed process $X_0(t) = X(\gamma^{-1}(t))$, where we used $\gamma(t) = l(t)/l(1)$. The Fourier coefficients are

$$\begin{aligned} A_s &= \sqrt{2} \int_0^1 X_0(t) \cos(2\pi st) dt \\ &= \sqrt{2} \int_0^1 X(t) \cos(2\pi s\gamma(t))\gamma'(t) dt, \end{aligned} \quad (4.1)$$

and the expression for B_s is similar.

It remains to fit the regression model (3.3), based on $A_s, B_s, s \geq 3$. The Fourier coefficients at high phases are poorly determined due to digitization effects, cf. e.g. [6, 7, 10]. We therefore considered the well-determined Fourier coefficients $A_3, B_3, \dots, A_S, B_S$ only, where S is a reasonable cut-off value. In practice it turned

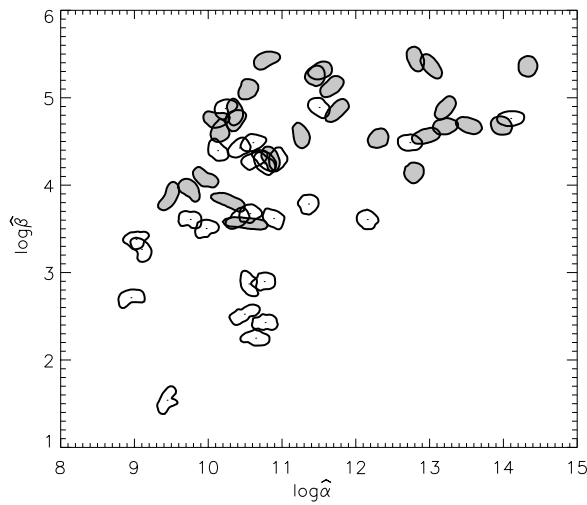


Figure 5. The estimates of (α, β) when p is fixed at $p = 2.5$. The hatched nuclei are from the benign sample while the white nuclei are from the malignant sample.

out that relatively few Fourier coefficients are well-determined and we used $S = 11$. Since the Fourier coefficients are zero mean Gaussian it follows that the likelihood function for a profile is

$$L(\alpha, \beta, p) = \prod_{s=3}^S \frac{1}{2\pi\lambda_s} \exp\left(-\frac{A_s^2 + B_s^2}{2\lambda_s}\right), \quad (4.2)$$

where λ_s is given by (3.3).

For each profile we found the estimates of (α, β, p) by maximising (4.2). For the malignant sample the average of p was 2.72 with a standard deviation of 0.68, while for the benign sample the average was 2.49 and the standard deviation 0.79. We therefore fixed $p = 2.5$. The estimates of (α, β) under the p -order model with $p = 2.5$ are shown in Fig. 5 and summarized in Table 1. The estimates of the local shape parameter β are on average significantly lower in the malignant sample (p -value for identical β s in the two

Table 1. The average, standard deviation and correlation of $(\log \hat{\alpha}, \log \hat{\beta})$ for each sample.

	$\log \hat{\alpha}$		$\log \hat{\beta}$		corr.
	av.	s.d.	av.	s.d.	
Benign	11.59	1.42	4.68	0.53	0.43
Malignant	10.65	1.10	3.66	0.88	0.45

samples is less than 0.01%). This was to be expected from the simulations and geometric interpretation of β given in Section 3.

On average the estimates of the global shape parameter α are also lowest in the malignant sample, and again the difference is significant (p -value close to 1%). Furthermore the variance of $\log \beta$ is significantly larger in the malignant sample.

Based on considerations from discriminant analysis, estimates like those presented in Table 1 can be used to judge questions of how many cells from a single tumour should be analysed in order to diagnose it as benign or malignant.

Appendix

Let $Y_1 \sim N(a, \lambda)$ and $Y_2 \sim N(b, \lambda)$ be independent random variables and let

$$a = l \cos \mu, \quad b = l \sin \mu, \\ Y_1 = R \cos \Theta, \quad Y_2 = R \sin \Theta.$$

We show that

$$\Theta \mid R = r \sim vM\left(\mu, \frac{lr}{\lambda}\right).$$

From the change of variables formula it follows that the density function of (R, Θ) is

$$f_{R,\Theta}(r, \theta) = \frac{r}{2\pi\lambda} \exp\left(\frac{-r^2 - l^2 + 2lr \cos(\theta - \mu)}{2\lambda}\right),$$

and by integrating with respect to θ we get

$$f_R(r) = \frac{r}{\lambda} \exp\left(\frac{-r^2 - l^2}{2\lambda}\right) I_0\left(\frac{lr}{\lambda}\right),$$

where I_0 denotes the modified Bessel function of the first kind and order 0. The result now follows immediately.

Acknowledgments

We would like to thank the two anonymous referees for helpful suggestions. The data has kindly been supplied by Professor Flemming Sørensen, Institute of Pathology, University of Aarhus. This work is supported in part by MaPhySto, funded by a grant from the Danish National Research Foundation. The second author is

supported by a grant from the Danish Natural Science Research Council.

References

1. A. Fitzgibbon, M. Pilu, and R.B. Fisher, "Direct least square fitting of ellipses," *IEEE Transactions on Pattern Analysis and Machine Intelligence*, Vol. 21, pp. 476–480, 1999.
2. U. Grenander, *General Pattern Theory*, Oxford University Press: New York, 1993.
3. U. Grenander and K.M. Manbeck, "A stochastic model for defect detection in potatoes," *Journal of Computer Graphics and Statistics*, Vol. 2, pp. 131–151, 1993.
4. U. Grenander and M.I. Miller, "Representations of knowledge in complex systems (with discussion)," *Journal of the Royal Statistical Society, B*, Vol. 56, pp. 549–603, 1994.
5. A. Hobolth and E.B.V. Jensen, "Modelling stochastic changes in curve shape, with an application to cancer diagnostics," *Advances in Applied Probability (SGSA)*, Vol. 32, pp. 344–362, 2000.
6. A. Hobolth, J.T. Kent, and I.L. Dryden, "On the relation between edge and vertex modelling in shape analysis," *Scandinavian Journal of Statistics*, Vol. 29, pp. 355–374, 2002.
7. A. Hobolth, J. Pedersen, and E.B.V. Jensen, "A continuous parametric shape model," Research Report no. 13, Laboratory for Computational Stochastics, University of Aarhus, submitted, 2000.
8. J.L. Jensen, "A large deviation-type approximation for the "Box class" of likelihood ratio criteria," *Journal of the American Statistical Association*, Vol. 86, pp. 437–440, 1991.
9. N.L. Johnson and S. Kotz, *Continuous Univariate Distributions—1*, Houghton Mifflin Company: Boston, 1970.
10. J.T. Kent, I.L. Dryden, and C.R. Anderson, "Using circulant symmetry to model featureless objects," *Biometrika*, Vol. 87, pp. 527–544, 2000.
11. K.V. Mardia and P.E. Jupp, *Directional Statistics*, Wiley: Chichester, 2000.
12. L.C.G. Rogers and D. Williams, *Diffusions, Markov Processes and Martingales*, Vol. 2, Wiley: Chichester, 2000.
13. H. Rue and M.A. Hurn, "Bayesian object recognition," *Biometrika*, Vol. 86, pp. 649–660, 1999.
14. H. Rue and A.R. Syversveen, "Bayesian object recognition with Baddeley's delta loss," *Advances in Applied Probability (SGSA)*, Vol. 30, pp. 64–84, 1998.
15. D. Stoyan and H. Stoyan, *Fractals, Random Shapes and Point Fields*, Wiley: Chichester, 1994.
16. C.T. Zahn and R.Z. Roskies, "Fourier descriptors for plane closed curves," *IEEE Transactions on Computers*, Vol. 21, pp. 269–281, 1972.



Asger Hobolth received the Ph.D. degree from the University of Aarhus in 2002. Currently he is at the Bioinformatics research centre at the University of Aarhus. His research interests are in shape analysis and medical imaging.



Jan Pedersen received the Ph.D. degree in mathematical statistics at the Department of Mathematical Sciences, University of Aarhus, in 1996. Since 2001 he has been an associate professor at the same institution. His main research interest are applications of stochastic processes.



Eva B. Vedel Jensen is professor in mathematical statistics of the Department of Mathematical Sciences at University of Aarhus. She is the scientific director of Laboratory for Computational Stochastics and coordinator of the interdisciplinary training site Advanced Medical Imaging and Spatial Statistics (MISS). Her research interests are in stochastic geometry, spatial statistics and computational stochastics.